

PROPERTIES OF THE VIRIAL EXPANSION AND EQUATION OF STATE OF IDEAL QUANTUM GASES IN ARBITRARY DIMENSIONS

KÅRE OLAUSSEN AND ASLE SUDBØ

Dedicated to Johan S. Høye on the occasion of his 70th birthday

ABSTRACT. The virial expansion of ideal quantum gases reveals some interesting and amusing properties when considered as a function of dimensionality d . In particular, the convergence radius $\rho_c(d)$ of the expansion is particularly large at *exactly* $d = 3$ dimensions, $\rho_c(3) = 7.1068\dots \times \lim_{d \rightarrow 3} \rho_c(d)$. The same phenomenon occurs in a few other special (non-integer) dimensions. We explain the origin of these facts, and discuss more generally the structure of singularities governing the asymptotic behavior of the ideal gas virial expansion.

1. INTRODUCTION

To cite an authoritative source, *the treatment of Bose-Einstein and Fermi-Dirac perfect gases can be made in an extremely simple manner* [1]. The topic has been known since the discovery of quantum statistics [2–5]. One might think that from a theoretical perspective there is absolutely nothing new to discover about it. Nonetheless, in this paper we report some rather amusing behavior found when investigating how the virial expansion and other properties depend on dimensionality d of the system. Here, d is an effective dimension given by $d = 2D/\nu$, where D is the dimension of physical space and ν is the power of wave number entering the dispersion relation of the excitations in question (see below). For nonrelativistic massive particles, we have $d = D$. For massless fermions (a reasonable description of neutrinos and electrons in topological insulators), we have $d = 6$, and for the asymptotic low-energy spectrum of electrons in graphene, we have $d = 4$. Moreover Bose-Einstein condensates with effective spatial dimensions D ranging from 0 to 3 are now routinely made. Such systems are of considerable current interest. While interactions obviously play a role to varying degrees in the above mentioned systems, this has nevertheless motivated us to revisit the behavior of ideal quantum gases as a function of dimensionality with an emphasis on the analytical structure of the equations of state and other thermodynamical quantities. The analytical structure reveals itself as surprisingly intricate and complex as dimension is varied.

For any dimension d the equation of state of an ideal quantum gas has a nonzero radius of convergence at $\rho = 0$. It can therefore be analytically continued to a complete Riemann surface with much (d -dependent) mathematically interesting structure. We have

Date: May 8, 2014: Published in *Transactions of The Royal Norwegian Society of Sciences and Letters*, 2014(3) 115–135.

Key words and phrases. Quantum statistical mechanics (05.30.-d), of quantum fluids (67.10.Fj), Equations of state gases (51.30.+i).

investigated how and where singularities occur on this Riemann surface, how they change character and position with changing d , and how that governs the asymptotic behavior of virial coefficients. We have even found cases where the analytically continued equation of state reappears in a new form, meaningful from the requirements that both density ρ and pressure p are real for physical values of the chemical potential μ (but usually pathological with regard to more detailed physical behavior). To our knowledge this has not previously been reported in the literature. [6]

An ideal Bose gas undergoes a condensation in which the zero-momentum ground state becomes macroscopically occupied above a critical density (or theoretically equivalent below a critical temperature) provided the dimensionality $d > 2$. This is a phenomenon accompanied by true non-analyticities in thermodynamic potentials (however without the appearance of collective modes). One would then expect on general grounds that any expansion of physical quantities (e.g. pressure) in powers of density would have a convergence radius given by the critical density or smaller.

On the other hand, it has been known for a long time that the virial expansion of an ideal non-relativistic Bose gas in $d = 3$ dimensions possesses the peculiar and somewhat surprising property of having a convergence radius $\rho_c(3)$ which is much larger than the critical density for Bose–Einstein condensation, $\rho_{\text{BE}}(3) = \zeta(\frac{3}{2})\Lambda_T^{-3}$ (where Λ_T is the thermal de Broglie wavelength, and ζ is the Riemann zeta function).

This was first demonstrated by Fuchs [7], following a conjecture by Widom [8]. Jensen and Hemmer [9] (see also Ziff and Kincaid [10]) estimated that $\rho_c(3) \approx 7 \times \rho_{\text{BE}}(3)$, based on numerical evaluation of the first 116 virial coefficients. The computation is by no means a trivial one — the n 'th virial coefficient has a magnitude of order $10^{-1.27n}$, the remainder of cancellations between terms of order 1. A reliable evaluation of the 116'th coefficient required computations to be carried out to 160 digits accuracy — a quite formidable task in 1971. In the above works, the reason for the existence of such a surprisingly large convergence radius was not discussed.

In $d = 2$ dimensions the situation is the opposite, $\rho_{\text{BE}}(2)$ is infinite while $\rho_c(2) = 2\pi\Lambda_T^{-2}$ (as can be seen from the repeatedly discovered exact virial expansion in two dimensions [10–13]). This led us to investigate the dependence on dimensionality in more detail. This had previously been done by Ziff and Kincaid [10] (they focused on integer dimensions only, but some of their results are valid for arbitrary dimensions). Actually, our parameter d need not correspond to the physical dimension of the system — what matters is that the density of states per energy interval scales like

$$g(\varepsilon) \sim \varepsilon^{d/2-1}, \quad (1.1)$$

and that it is possible to define pressure and density as position independent quantities. For excitations with dispersion relation $\varepsilon(\mathbf{p}) \sim |\mathbf{p}|^\nu$ in D physical dimensions we find $d = 2D/\nu$. Only for a standard nonrelativistic spectrum will d correspond to the physical dimension. With excitations living on a fractal subset of physical space we may also obtain a non-integer d . Although there may be many interesting physical realizations, the purpose of varying d continuously in this paper is mainly to obtain a more coherent and connected picture of the behavior of the virial expansion as dimensionality is varied.

The rest of this paper is organized as follows. In Section 2 we first discuss a peculiar symmetry between fermions and bosons which occur in the case of ideal quantum gases, its

origin, and how it extends to interacting systems. Next we discuss some general aspects of the virial expansion, and display the first few term of the ideal Bose gas expansion for general dimension d .

Section 3 describes our numerical exploration of the virial coefficients A_n as function of dimension d . Each A_n has a number of zeros. They reveal intriguing patterns which inspired many conjectures (and eventually this whole research).

In Section 4 we consider the special cases of $d = 0$ (quantum dot), $d = 2$ (confined layer), and $d = 3$. Apart from their physical applications, $d = 0$ and 2 are interesting since in those cases the relation between fugacity z and density ρ can be inverted exactly. Hence, they allow for a more explicit and detailed analysis, and provide boundary conditions which must be obeyed by the general expansions. The physically most important system, $d = 3$, is peculiar in that the equation of state (i.e., pressure p as function of ρ) extends analytically beyond the density ρ_{BE} for Bose-Einstein condensation. This analytic behavior also holds for other thermodynamic quantities like the chemical potential (the density fluctuations exhibit a pole singularity at ρ_{BE}). The behavior for $\rho > \rho_{\text{BE}}$ is easily seen to be unphysical, and is not related to the correct behavior of the condensed state.

Section 5 is a mathematical discussion of how the parametric representation (2.2) can be extended to the Riemann surface of the polylogarithmic functions involved, leading to the general parametric representation (5.7). The sheets of the complete Riemann surface are labeled by an infinite-dimensional vector \mathbf{k} of integers. On an infinite subset of these sheets the parametric representation (5.7) provide a candidate equation of state, related to the usual (low-density) Bose equation of state by analytic continuation.

Section 6 is a first account of our travel on the Riemann surface of the equation of state, first locating the singularities governing the radius of convergence of the virial expansion for $d = 3$, and next exploring how these singularities move as d is changed.

In Section 7 we demonstrate how knowledge of the closest singularities of $p(\rho)$, and the behavior of $p(\rho)$ around these, can be used to provide an accurate analytical representation of the asymptotic behavior of the virial coefficients. The analytic prediction compares very well with numerically calculated coefficients.

In Section 8 the behavior near the Bose-Einstein condensation point is analysed, revealing why the singularity in the equation of state vanishes at this point for dimensions $d = 2 + 2/(m + 1)$ (with $m = 1 \dots 6$).

Section 9 is a second account of our exploration of the Riemann surface, with focus on how singularities of the equation of state flow when d is changed, and in particular the behavior of this flow as $d \rightarrow 2$ and $d \rightarrow 0$. The singularities are in general of square root type. However, for $d = 2$ the singularities are logarithmic; hence each of them must be formed by an infinite number of coalescing square root singularities as $d \rightarrow 2$. Moreover, (infinitely) many pairs of square root singularities flow towards $\rho = 0$ as $d \rightarrow 0$, where none can be seen in the explicit equation of state. The annihilation mechanism seems to be similar to the one which is operative in the disappearance of two square root singularities in $\sqrt{z^2 - \varepsilon^2}$ when $\varepsilon \rightarrow 0$.

We close the paper with a few remarks in Section 10.

2. VIRIAL EXPANSIONS FOR IDEAL QUANTUM GASES

Consider a d -dimensional volume $V = L^d$ filled with identical nonrelativistic, noninteracting mass- m quantum mechanical particles. Without internal degrees of freedom, the number of single-particle states in a tiny interval $d\varepsilon$ around ε is

$$\frac{V}{\Gamma(d/2)} \left(\frac{2\pi m\varepsilon}{h^2} \right)^{d/2} \frac{d\varepsilon}{\varepsilon} \equiv V g(\varepsilon) d\varepsilon \quad (2.1)$$

when $\varepsilon > 0$ (otherwise zero). Here, the surface of a unit sphere in d dimensions is set to $S_{d-1} = 2\pi^{d/2}/\Gamma(d/2)$ in general, and we have assumed that $V \rightarrow \infty$ in a regular manner. At a given temperature T we choose to measure energy in units of $k_B T$, and length in units of the thermal wavelength $\Lambda_T = (2\pi m k_B T/h^2)^{-1/2}$. For bosons in the grand canonical ensemble the equation of state is given in implicit form by

$$p = \frac{1}{\Gamma(1+d/2)} \int_0^\infty \frac{d\varepsilon}{\varepsilon} z \varepsilon^{1+d/2} \frac{1}{e^\varepsilon - z}, \quad (2.2)$$

$$\rho = \frac{1}{\Gamma(d/2)} \int_0^\infty \frac{d\varepsilon}{\varepsilon} z \varepsilon^{d/2} \frac{1}{e^\varepsilon - z},$$

where $z = e^\mu$ is the fugacity and μ the chemical potential. The expressions for fermions are the same with the replacements

$$\rho \rightarrow -\rho, \quad z \rightarrow -z, \quad p \rightarrow -p. \quad (2.3)$$

It is intriguing that the *same* functions describe both bosons and fermions, only in different parameter ranges.

However, the generalization of equation (2.3) to interacting systems is less direct. In a functional integral formalism, the fugacity relation between bosons and fermions is related to the rule that for bosons one should integrate over classical fields φ which are periodic in the imaginary time (τ) direction, and for fermions over Grassmann fields χ which are antiperiodic. This difference can be eliminated by a τ -dependent gauge transformation at the cost of transforming $\mu \rightarrow \mu + (2n+1)\pi i$, equivalent to $z \rightarrow -z$. Without interactions the relation between pressures p is a consequence of the relation between classical and Grassmann gaussian integrals,

$$e^{pV} = \int \mathcal{D}\varphi^* \mathcal{D}\varphi e^{-\varphi^* A \varphi} \propto \det^{-1} A,$$

$$e^{pV} = \int \mathcal{D}\chi^* \mathcal{D}\chi e^{-\chi^* A \chi} \propto \det A,$$

which in the interacting case generalizes to the diagrammatic rule of one extra minus-sign per fermion loop. I.e., if we for a model with interactions know the complete loop expansion of the bosonic functional integral, with $p_L(z)$ being the L -loop contribution, then relation (2.3) generalized to

$$p_f(z) = \sum_L (-1)^{fL} p_L((-1)^f z), \quad \rho_f(z) = z \frac{d}{dz} p_f(z), \quad (2.4)$$

where $f = 0$ for bosons and $f = 1$ for fermions.

In the following, we return to the noninteracting model and we will mainly consider bosons in explicit expressions. The integrals (2.2) can be written as power series in z (Mayer expansions),

$$\begin{aligned} p &= z + \sum_{\ell=2}^{\infty} \frac{z^{\ell}}{\ell^{1+d/2}} \equiv z + \sum_{\ell=2}^{\infty} b_{\ell} z^{\ell}, \\ \rho &= z + \sum_{\ell=2}^{\infty} \frac{z^{\ell}}{\ell^{d/2}} = z + \sum_{\ell=2}^{\infty} \ell b_{\ell} z^{\ell}. \end{aligned} \quad (2.5)$$

The fermion expressions are obtained by $b_{\ell} \rightarrow (-)^{\ell+1} b_{\ell}$. By eliminating z and expressing p in terms of ρ we obtain the virial expansion,

$$p = \rho + \sum_{n=2}^{\infty} A_n \rho^n, \quad (2.6)$$

where A_n are the virial coefficients. The fermion coefficients are related to the bosonic ones by $A_n \rightarrow (-1)^{n+1} A_n$. Therefore, the bosons and fermions have the same radius of convergence for their virial expansions, governed by singularities which are related by inversion, $\rho \rightarrow -\rho$. Due to reality conditions both cases also have reflection symmetry under $\text{Im } \rho \rightarrow -\text{Im } \rho$. Thus, singularities outside the real axis will occur in complex conjugate pairs.

The virial coefficients can be calculated by order-by-order inversion of the Mayer series (2.5). They can also be found through an explicit algorithm [14]. For the latter, define the power series

$$g(z) = \sum_{\ell=1}^{\infty} (\ell+1) b_{\ell+1} z^{\ell}, \quad (2.7)$$

and coefficients C_{nm} through the generating function

$$\frac{t g(z)}{1 + t g(z)} = - \sum_{n=1}^{\infty} \sum_{m=1}^n C_{nm} z^n t^m. \quad (2.8)$$

An alternative way to describe C_{nm} is as follows: Define $v_n = -(n+1)b_{n+1}$. Then

$$C_{nm} = \sum' \left(\nu_1 \nu_2 \nu_3 \cdots \right) v_1^{\nu_1} v_2^{\nu_2} v_3^{\nu_3} \cdots$$

where the sum is over all sets $\{\nu_1 \nu_2 \nu_3 \cdots\}$ of non-negative integers such that $\sum_k \nu_k = m$ and $\sum_k k \nu_k = n$. In any case the virial coefficients are

$$A_{n+1} = \frac{1}{n+1} \sum_{m=1}^n \binom{n+m-1}{m} C_{nm}. \quad (2.9)$$

Likewise, the fugacity can be expressed in terms of density as

$$z = \rho + \sum_{n=2}^{\infty} B_n \rho^n, \quad (2.10)$$

where

$$B_{n+1} = \frac{1}{n+1} \sum_{m=1}^n \binom{n+m}{m} C_{nm}. \quad (2.11)$$

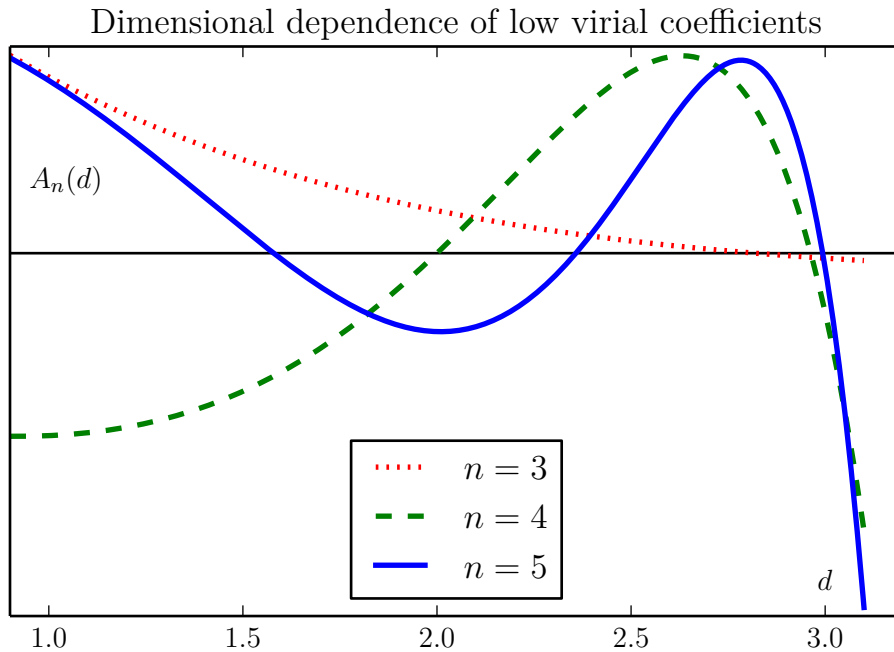


FIGURE 1. The 3rd to 5th virial coefficients as function of dimension d . To adjust all curves to the same plot we have multiplied A_n by expressions $e^{\alpha+\beta d}$, with real n -dependent coefficients α and β . Note that $A_n(d)$ has a zero which rapidly approaches $d = 3$ as n increases.

The first virial coefficients are explicitly (with $x = 1 + d/2$),

$$\begin{aligned}
 A_2(d) &= -2^{-x}, \\
 A_3(d) &= 4 \cdot 4^{-x} - 2 \cdot 3^{-x}, \\
 A_4(d) &= -20 \cdot 8^{-x} + 18 \cdot 6^{-x} - 3 \cdot 4^{-x}, \\
 A_5(d) &= 112 \cdot 16^{-x} - 144 \cdot 12^{-x} + \\
 &\quad 18 \cdot 9^{-x} + 32 \cdot 8^{-x} - 4 \cdot 5^{-x}.
 \end{aligned} \tag{2.12}$$

They are plotted in figure 1. Fermion coefficients are obtained by $A_n \rightarrow (-1)^{n+1} A_n$.

3. NUMERICAL EXPERIMENTS

The virial coefficients (2.12) exhibit much structure when analysed as function of dimensionality. They reveal an interesting pattern of zeros. The most prominent feature is that one zero $d_1(n)$ rapidly approaches $d = 3$ as n increases, and another $d_2(n)$ rapidly approaches $d = \frac{8}{3}$. Numerically, we find

$$3 - d_1(n) = 2 \cdot 10^{-1}, 4 \cdot 10^{-2}, 6 \cdot 10^{-3}, 7 \cdot 10^{-4}, \dots \tag{3.1}$$

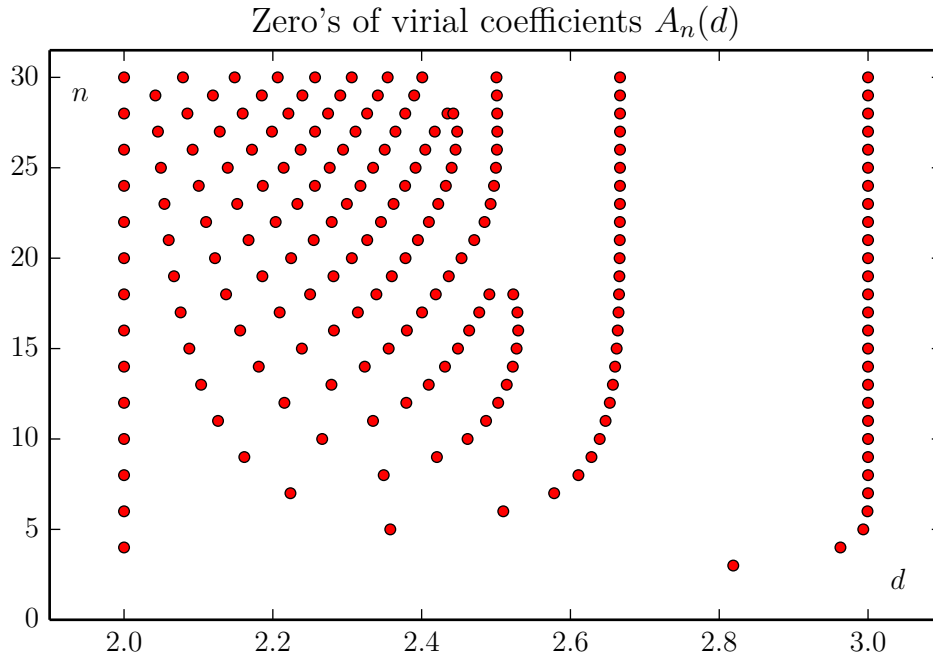


FIGURE 2. Scatter plot of the zero's of the virial coefficients $A_n(d)$ in the region $2 \leq d$ for $3 \leq n \leq 30$. There are additional zeros in the region $d < 2$.

for $n = 3, 4, \dots$. The convergence turns out to be exponential in n , with some oscillations in the prefactor. Clearly, it is the presence of the zeros close to $d = 3$ which causes the virial expansion to have an unusually large radius of convergence at $d = 3$.

More generally, the set of zeros form an intriguing pattern at low n . Investigating this order by order is an amusing numerical experiment, providing many opportunities to make (wrong) conjectures. When extending this experiment up to $n = 300$, we found the most prominent features to be that i) at $d = 2$ all even virial coefficients beyond the second vanish, $A_{2n}(2) = 0$ for $n = 2, 3, \dots$, and ii) there are several special dimensions d_m which act as “attractors” for zeros, with the consequence that the virial expansion has an exceptionally large convergence radius, $\rho_c(d_m) > \rho_{BC}(d_m)$, for such dimensions.

We soon discovered that the special dimensions followed the pattern

$$d_m = 2 + \frac{2}{m+1}, \quad m = 1, 2, \dots, \quad (3.2)$$

leading to the conjecture that this is true for all m . The correct result, which is difficult to discover by numerical experiments alone, is that equation (3.2) holds only for $m = 1, 2, \dots, 6$. The first 5 members of this set are clearly visible as the emerging lines in Fig. 3.

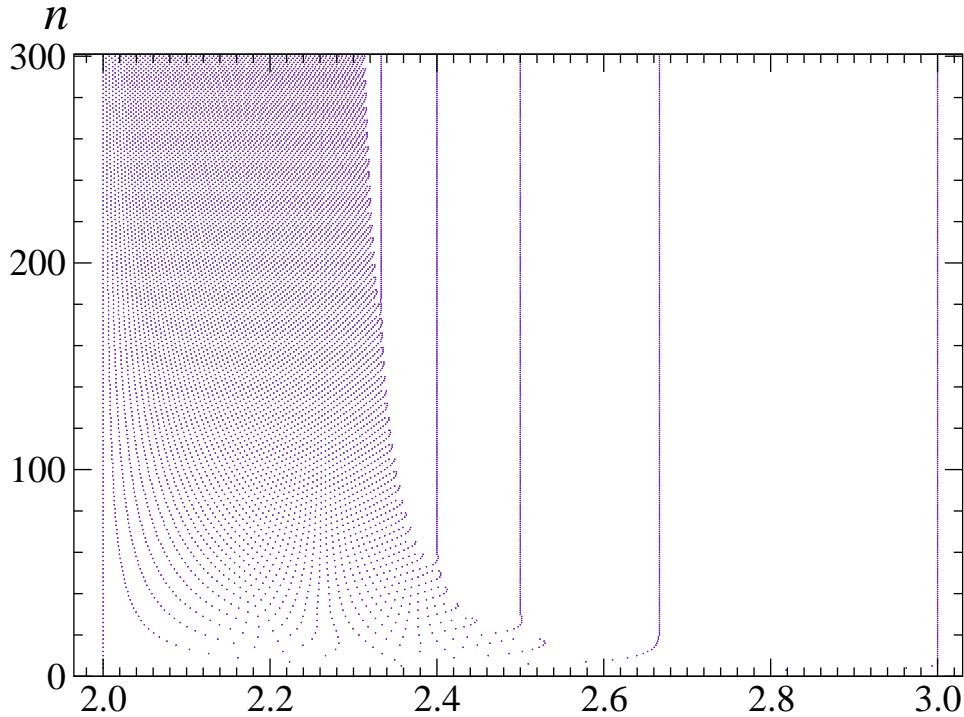


FIGURE 3. Scatter plot of the zero's of the virial coefficients $A_n(d)$ in the region $2 \leq d$, $3 \leq n \leq 300$. There are additional zeros in the region $d < 2$.

4. SPECIAL DIMENSIONS

We next consider some special cases of d . The expressions (2.5) can be analysed completely when $d = 0$ and $d = 2$.

4.1. Quantum dot. For $d = 0$ we find $\rho = z/(1 - z)$ and $p = -\ln(1 - z)$. I.e.

$$p = \ln(1 + \rho) = \rho + \sum_{n=2}^{\infty} \frac{(-1)^{n+1}}{n} \rho^n, \quad (4.1)$$

with virial coefficients $A_n = (-1)^{n+1}/n$ and radius of convergence $\rho_c(0) = 1$ due to the logarithmic singularity at $\rho = -1$. This singularity has no natural physical interpretation for bosons. However, it corresponds to the maximum obtainable density for fermions. The $d = 0$ fermionic equation of state is the same as for a classical hard core lattice gas (without other interactions).

4.2. Two-dimensional layer. For $d = 2$, we find $\rho = -\ln(1 - z)$ and can infer the differential equation $(dp/d\rho) = \rho/(e^\rho - 1)$ with $p(0) = 0$. The solution is

$$p = \int_0^\rho \frac{dt t}{e^t - 1} = \text{dilog}(e^{-\rho}). \quad (4.2)$$

Note that $\text{dilog}(e^\rho) = -\frac{1}{2}\rho^2 - \text{dilog}(e^{-\rho})$, as can be verified by direct manipulation of the integral. Thus, the equation of state for fermions and bosons only differ in the second

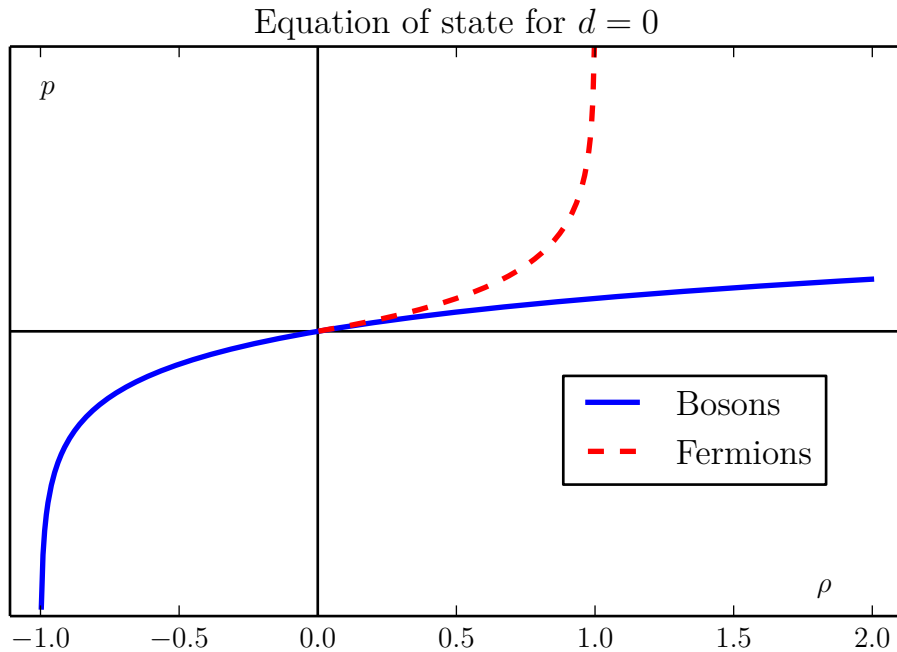


FIGURE 4. The equation of state for ideal quantum gases in zero dimensions. The boson equation of state in its unphysical third quadrant ($\rho < 0$, $p < 0$) actually describes the fermion equation of state in its physical region, obtained by inversion about the origin as shown. This is a general feature of noninteracting systems in any dimension.

virial coefficient, $p_{\text{fermion}} = p_{\text{boson}} + \frac{1}{2}\rho^2$. This can also be seen from the explicit virial coefficients, $A_n = B_{n-1}/n!$ where B_n are the Bernoulli numbers. Since $B_n = 0$ for all odd $n > 1$ the virial coefficients $A_n = 0$ for all even $n > 2$ (recall that all odd coefficients are equal for bosons and fermions). The property that only the second virial coefficient depends on statistics seems to generalize to Haldane exclusion statistics [15] (interpolating between bosons and fermions) in two dimensions [16]. The requirements, beyond interpretation of exclusion statistics, are that i) the density of states is constant as function of energy, and ii) a position-independent pressure and density can be defined. The latter condition is not fulfilled by the Hamiltonian model considered in Ref. 16, see Ref. 17, but this does not affect their computation of virial coefficients.

Due to pole singularities in the integrand at $t = 2\pi in$ (with integer $n \neq 0$) the function $p(\rho)$ has logarithmic singularities at the same points. Hence, the virial expansion has a radius of convergence, $\rho_c(2) = 2\pi$. We know of no physical reasons for the occurrence of these singularities (contrary to the $d = 0$ case, where the singularity has a physical origin in the fermion system).

For later analysis, recall that a logarithmic singularity has infinitely many Riemann sheets. In this case, when ρ encircles the singularity at $2\pi im$ once in the clockwise direction

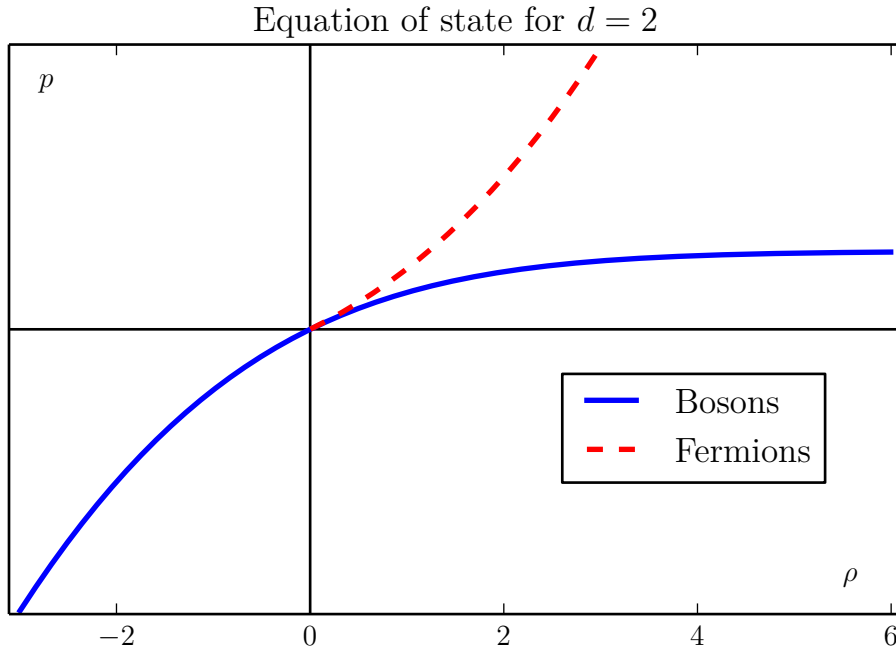


FIGURE 5. The equation of state for ideal quantum gases in two dimensions. The boson and fermion equations of state only differ in their second virial coefficient. Two space dimensions allow for intermediate (anyon) statistics which interpolates between the bosons and fermions. The equation of state for such hypothetical particles is not exactly known, and probably very far from a smooth interpolation at high densities (equivalent to low temperatures).

the function changes by $p \rightarrow p - 4\pi^2 m$. The result of repeated encirclings is that

$$p \rightarrow p - 4\pi^2 \sum_m m k_m \quad (4.3)$$

when the singularity at $\rho = 2\pi i m$ is encircled k_m times in total, counted in the clockwise direction. The order in which the encirclings occur does not matter. Hence, in the two-dimensional ($d = 2$) case, each Riemann sheet is uniquely labeled by a single integer $N = \sum_m m k_m$. The total surface is multiply connected, so there are infinitely many topologically inequivalent ways of moving from one sheet to another. Amusingly, the *same* Mayer expansion (2.5) (for $d = 2$) defines an infinity of possible equations of state, depending on which Riemann sheet is selected. All these equations of state are physical in the sense that the pressure is real when the density is real.

As will be seen in Section 5 this behavior extends to all dimensions d , with the generalization that each Riemann sheet is labeled by an infinite-dimensional vector \mathbf{k} of integers, which generically must be restricted by the condition $k_m = -k_{-m}$ for the pressure to be real when the density is real.

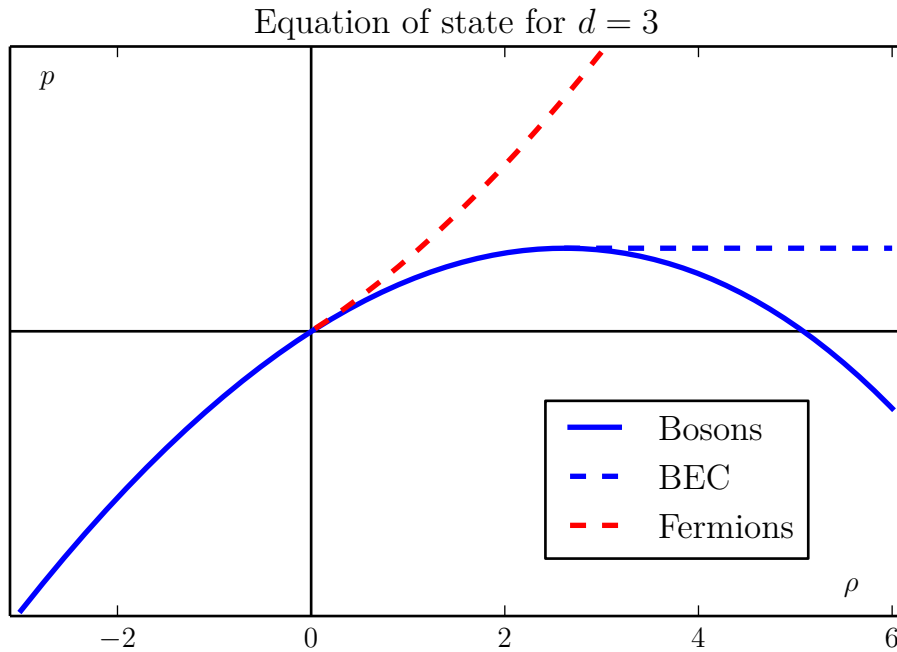


FIGURE 6. The equation of state for ideal quantum gases in three dimensions. The pressure as a function of density can be analytically continued beyond the critical density for Bose-Einstein condensation, $\rho_{\text{BE}} = \zeta(\frac{3}{2}) = 2.612\dots$. The same is true for other thermodynamic quantities, like the chemical potential $\mu = \mu(\rho)$. However, the behavior for $\rho > \rho_{\text{BE}}$ is unphysical (with $(dp/d\rho) < 0$ and $(d\mu/d\rho) < 0$), and does not correspond to the correct infinite volume limit of the system.

4.3. Three dimensions. In three dimensions, it seems impossible to invert the Mayer expansion (2.5) explicitly. We have evaluated $A_n(3)$ numerically to high accuracy and quite large n . They behave like

$$A_n(3) \sim \mathcal{A}(n) \exp(-an) \cos(bn + c) \quad (4.4)$$

when n becomes large. Here $\mathcal{A}(n)$ changes quite slowly and smoothly (i.e. algebraically) with n , and $a \approx 2.9$, $b \approx 0.7$. As shown in Fig. 6 an equation of state can be computed from this virial expansion far beyond the Bose-Einstein condensation point $\rho_{\text{BE}} = \zeta(\frac{3}{2}) \approx 2.612\dots$. However, the solid curve is unphysical for $\rho > \rho_{\text{BE}}$, since pressure decreases with increasing density.

In general, the virial coefficients can be expressed by a contour integral

$$A_n = \int_{\mathcal{C}} \frac{d\rho}{2\pi i} \frac{p(\rho)}{\rho^{n+1}}. \quad (4.5)$$

For evaluation at large n one should deform the closed curve \mathcal{C} as far away from the origin as possible, since the behavior of A_n then is governed by the contributions from the nearest singularities of $p(\rho)$, beyond which \mathcal{C} cannot be deformed. With a pair of complex conjugate

singularities, at $\rho_+ = \rho_c e^{i\omega}$ and $\rho_- = \rho_c e^{-i\omega}$, one obtains an asymptotic behavior

$$A_n \sim \rho_c^{-n} \cos(n\omega + \phi), \quad (4.6)$$

up to algebraic corrections in n . The phase ϕ is not important for locating the singularities. By comparing this result with the numerical observations, one concludes that the convergence of the $d = 3$ virial expansion is governed by a complex conjugate pair of singularities at $\rho_{\pm} \approx \exp(2.9 \pm 0.7i) \approx 18.5 \exp(\pm 0.7i) \approx 14 \pm 12i$. This is in agreement with earlier findings that the radius of convergence is much larger than the critical density for Bose-Einstein condensation. We want to study these singularities in more detail.

5. ANALYTIC CONTINUATION AND RIEMANN SURFACE

There are two possible sources of singularities in an implicitly represented function $p(\rho) = p(z(\rho))$, namely i) singularities which are explicit in the parametric representation of $p = p(z)$ or $\rho = \rho(z)$, or both (in which case they may sometimes compensate each other), and ii) singularities occurring where $\rho(z)$ is analytic, but cannot be inverted to an analytic function $z(\rho)$ because $d\rho(z)/dz = 0$. The singularities of relevance to our case are of the second kind. To find their accurate positions in the ρ -plane, and the corresponding z -plane values, one must extend the parametric representation (2.2) to the full Riemann surface of the functions involved.

The expressions involved are known as polylogarithmic functions,

$$\text{Li}_s(z) = \frac{1}{\Gamma(s)} \int_0^\infty \frac{d\varepsilon}{\varepsilon} \frac{z \varepsilon^s}{e^\varepsilon - z} = \sum_{n=1}^{\infty} \frac{z^n}{n^s}. \quad (5.1)$$

The sum converges for $|z| < 1$ and has an analytic extension equal to the integral expression in the whole z -plane cut along the real z -axis from 1 to ∞ . This is the primary Riemann sheet of the polylogarithm. Moving z along a closed path which winds once clockwise around $z = 1$ (not encircling $z = 0$) changes the integral so that

$$\text{Li}_s(z) \rightarrow \text{Li}_s(z) + \frac{2\pi i}{\Gamma(s)} (\log z)^{s-1}, \quad (5.2)$$

where the right hand side again is defined on the primary Riemann sheet. The new term arises because moving z across the positive real ε -axis drags the integration path with it. This can be undone by explicitly evaluating the pole contribution which makes up the difference. The new term must be handled carefully, since $\log z$ is multivalued around $z = 0$ and $(\log z)^{s-1}$ is multivalued around $z = 1$. We introduce $\mu \equiv \log z$ as a new variable, in terms of which the singularity at $z = 1$ becomes the image of infinitely many singularities in the μ -plane, at $2\pi i m$, $m = 0, \pm 1, \pm 2, \dots$. We define the primary Riemann sheet by introducing cuts $2\pi i m + x$, $0 \leq x \leq \infty$. If we start on the primary sheet and make k crossings (counted in the clockwise direction) of the cut from $2\pi i m$ to ∞ , and no crossings of any other cuts, the polylogarithm will change as

$$\begin{aligned} \text{Li}_s(e^\mu) &\rightarrow \text{Li}_s(e^\mu) \\ &+ \Gamma(1-s) \left(e^{2\pi i k(1-s)} - 1 \right) (2\pi i m - \mu)^{s-1}. \end{aligned} \quad (5.3)$$

This is found most safely from the expression [18],

$$\sum_{n=1}^{\infty} \frac{e^{n\mu}}{n^s} = \Gamma(1-s) (-\mu)^{s-1} + \sum_{n=0}^{\infty} \zeta(s-n) \frac{\mu^n}{n!}, \quad (5.4)$$

which is convergent in a finite region around $\mu = 0$. It can also be seen directly, in that each new crossing adds a new function, but also changes the phase of the previously emerged ones. Hence, the total contribution from k crossings is

$$\begin{aligned} & \frac{2\pi i}{\Gamma(s)} \sum_{n=0}^{k-1} e^{-2\pi i n(s-1)} (\ln z)^{s-1} \\ &= \frac{\pi}{\Gamma(s) \sin \pi(1-s)} \left(e^{2\pi i k(1-s)} - 1 \right) (e^{-\pi i} \ln z)^{s-1}. \end{aligned}$$

By paying close attention to phase relations on the primary sheet one finds $e^{-\pi i} \ln z = -\mu$. By further using the formula $\Gamma(t)\Gamma(1-t) = \pi / \sin \pi t$ one finds agreement with equation (5.3). This equation is also valid if k is negative, that is if one makes crossings in the anticlockwise direction.

The contributions from crossing different branch cuts are additive and do not interfere with each other. Thus, it does not matter in which order the various crossings have occurred, only their total number. This is a great simplification. Thus, we may label the Riemann sheets by an integer-valued vector \mathbf{k} , where k_m is the net number of times the branch cut from $2\pi i m$ to ∞ has been crossed in the clockwise direction (starting from the primary sheet), and define a polylogarithm extended to the complete Riemann surface as

$$\text{Li}(\mu, s; \mathbf{k}) = \text{Li}_s(e^\mu) + \sum_{m=-\infty}^{\infty} C(k_m, s) (2\pi i m - \mu)^{s-1}, \quad (5.5)$$

where

$$C(k, s) = \frac{2\pi i}{\Gamma(s)} \frac{\sin \pi k(1-s)}{\sin \pi(1-s)} e^{\pi i k(1-s)}. \quad (5.6)$$

When starting from the primary sheet, in practice only a few (if any) of the coefficients k_m will be nonzero. Equation (5.3) provides the analytically continued expressions for pressure and density,

$$\begin{aligned} p &= \text{Li}(\mu, 1 + d/2; \mathbf{k}), \\ \rho &= \text{Li}(\mu, d/2; \mathbf{k}). \end{aligned} \quad (5.7)$$

Note that $C(-k, s) = C(k, s)^*$. Therefore, p and ρ will be real when $k_m = -k_{-m}$ for all m , thereby making the relation between p and ρ a candidate for a physical bosonic equation of state (with the physical region defined by μ being real). Additional possibilities arise for rational values of s , when the logarithmic singularities at $\mu = 2\pi i m$ become algebraic and the coefficients C become periodic in k . Note that

$$\begin{aligned} C(k, m) &= (-1)^{m-1} \frac{2\pi i k}{(m-1)!} && \text{for } m = 1, 2, \dots, \\ C(k, -m) &= 0 && \text{for } m = 0, 1, \dots \end{aligned}$$

6. LOCATING THE SINGULARITES

It would be almost impossible to find the singularities of interest if one did not know where to look. Fortunately, we are in a situation quite similar to the one of explorers searching for a magnetic pole, in that we have a compass showing which direction to follow.

From the numerically calculated virial coefficients for $d = 3$, we conclude that the behavior is governed by the singularity at $\rho_+ \approx 14 + 12i$ and its complex conjugate. It is then easy to map out a path from the origin to ρ_+ by solving the equation $\rho(\mu(t)) = t\rho_+$ numerically and step by step for $t = \Delta t, 2\Delta t, \dots$. This leads to the Riemann sheet defined by $k_0 = 1$, all other $k_m = 0$. As t approaches 1, the inversion becomes difficult in accordance with our expectation that $\rho(z)$ cannot be inverted at the singularity, namely

$$\frac{d\rho}{dz} = \frac{1}{z} \text{Li}(\mu, -1 + d/2; \mathbf{k}) = 0. \quad (6.1)$$

One may then change the search algorithm to a direct solution of this equation, which is explicitly

$$-\sqrt{\frac{4\pi}{-\mu}} + \sum_{n=1}^{\infty} \frac{e^{n\mu}}{n^{1/2}} = 0. \quad (6.2)$$

This equation can be solved numerically to essentially arbitrary accuracy. We find

$$\begin{aligned} \mu_+ &= -0.322\,995\,155\,543\,097 - 6.618\,613\,424\,959\,805\,i, \\ z_+ &= 0.683\,629\,720\,405\,578 - 0.238\,314\,132\,061\,880\,i, \\ \rho_+ &= 14.074\,421\,676\,564\,36 + 12.107\,496\,215\,707\,89\,i \\ &= 18.565\,581\,330\,600\,061 e^{0.710\,413\,678\,806\,621\,i}. \end{aligned} \quad (6.3)$$

The results of Ref. 9 and 10 are in agreement with (6.3) to within the estimated accuracy.

A z -plane map of the journey described above, to the singularity at ρ_+ , is shown in Fig. 7 and described in the figure caption. The other journey follows the complex conjugate path. As shown, one has to cross two branch cuts in the complex z -plane. When the singularity first has been located it is very easy to follow its movement as one changes the dimension d . We discuss this in more detail in the captions to Fig. 7 and Fig. 8, and further in Section 9.

7. ASYMPTOTIC VIRIAL COEFFICIENTS

With accurate information on the singular behavior we may use (4.5) to compute the asymptotic behavior of A_n as $n \rightarrow \infty$. We may expand $\rho(\mu)$ and $p(\mu)$ around μ_+ , that is, with $\Delta\mu = \mu - \mu_+$, $\Delta\rho = \rho_+ - \rho$, and $\Delta p = p - p_+$, where

$$\Delta\rho = -\sum_{n=2}^{\infty} \frac{r_n}{n!} \Delta\mu^n, \quad \Delta p = \sum_{n=1}^{\infty} \frac{p_n}{n!} \Delta\mu^n. \quad (7.1)$$

Here, $p_n = r_{n-1} = \text{Li}(\mu_+, 1 - n + d/2; \mathbf{k})$. In particular, $p_1 = \rho_+$ and $p_2 = r_1 = 0$ (the singularity condition). We may now express $\Delta\mu$ order by order in $\Delta\rho$, thus

$$\begin{aligned} \Delta\mu &= (-2/r_2)^{1/2} \sqrt{\Delta\rho} + \dots, \\ \Delta p &= (-2/r_2)^{1/2} \rho_+ \sqrt{\Delta\rho} + \dots \end{aligned} \quad (7.2)$$

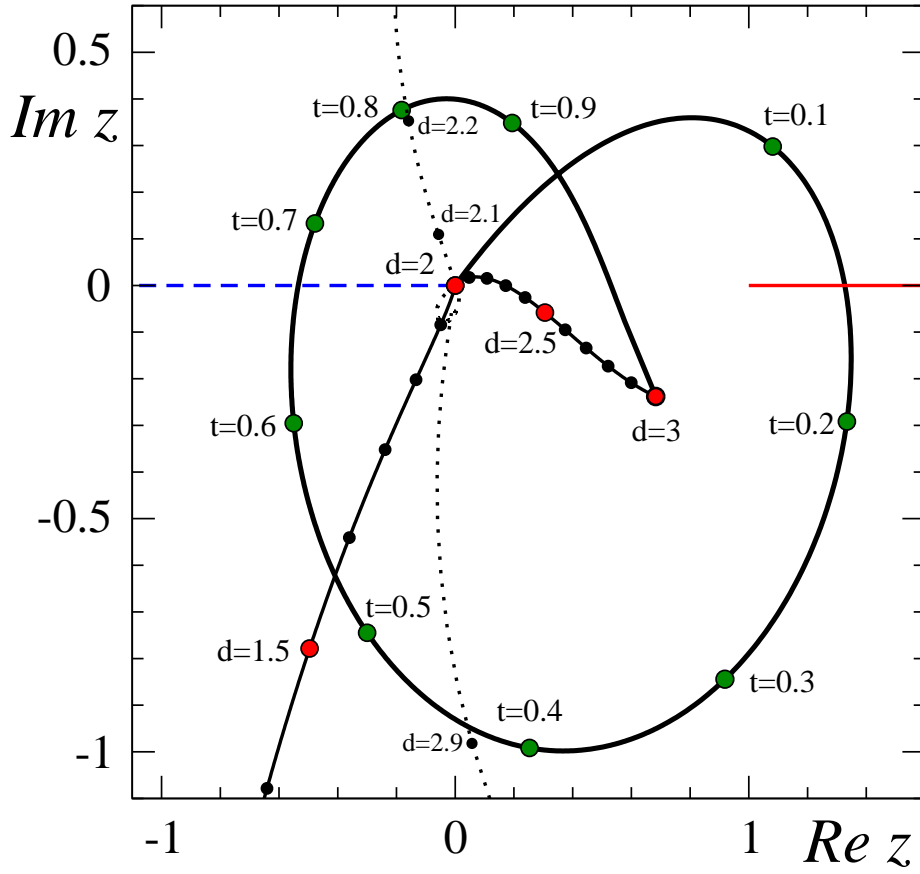


FIGURE 7. This figure maps our explorations of singularities. The fulldrawn line (colored red) is the first branch cut, running from $z = 1$ to $z = \infty$ along the positive real axis. The dashed line (colored blue) is the second branch cut, running from $z = -\infty$ to $z = 0$ along the negative real axis. We first found the (fulldrawn black) line in the z -plane which corresponds to the curve $\rho(t) = t\rho_+(3)$, $0 \leq t \leq 1$, starting at $z = 0$. The filled circles (colored green) mark the progression as t increases. As can be seen, one must cross two branch cuts before reaching the singularity $\rho_+(3)$.

Having found $\rho_+(3)$ and equation (6.1) determining $\rho_+(d)$, it is easy to explore how the singularity moves when one changes d . This is shown by the next fulldrawn (black) line. The black dots and filled circles (colored red) mark the progression as d decreases. When $d \rightarrow 0$ the singularity moves to $z = \infty$ (multiplied by a phase), corresponding to a singular point at $\rho = -1$. Actually, (6.1) becomes ambiguous when $d \rightarrow 2, 0, -2, \dots$. To handle this, we may write $d = 2 + \varepsilon e^{i\varphi}$ with ε a small positive number (0.001), and varied φ from 0 to π . In the z -plane the singularity moves slightly above $z = 0$ and back across the second branch cut. Alternatively, one may vary φ from 0 to an infinite number of other possible endpoints $(2k + 1)\pi$. Each choice leads to a different solution. There are infinitely many singularities approaching $\rho = 2\pi i$ as d approaches 2. We have mapped out several endpoint choices before decreasing d to 0 or increasing d back to 3. The two black dotted lines show how the singularity moves when the encircling is chosen to $\pm 2\pi$, and d is increased back to 3. See the caption to Fig. 8 for a further description.

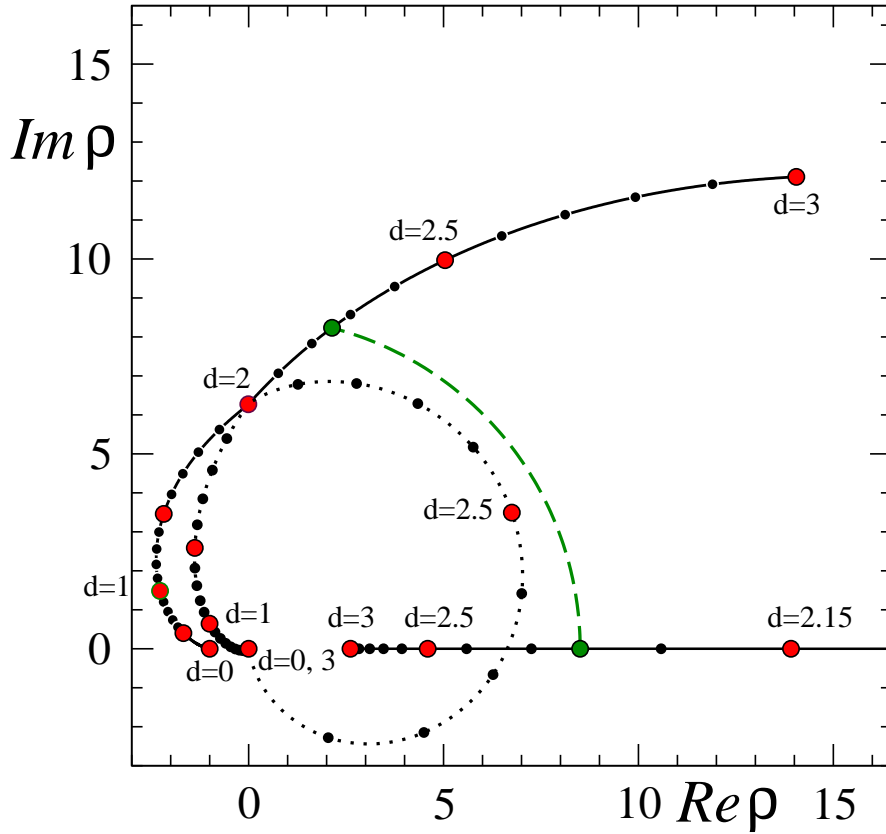


FIGURE 8. This figure shows how the singularities $\rho_+(d)$ and $\rho_{BE}(d)$ move as one changes the dimension d . Starting near $d = 3$ the singularity $\rho_{BE}(d)$ is closer to the origin than $\rho_+(d)$, thus determining the convergence radius of the virial expansion (except when d is equal to one of the special points d_m). However, as d decreases $\rho_+(d)$ moves inwards while $\rho_{BE}(d)$ moves outwards. Thus, there is a crossover dimension d_c , indicated by the filled circles (colored green), where they are equally far from the origin (as indicated by the green dashed circle). We find $d_c \approx 2.252563996$. For $d < d_c$ the convergence radius of the virial expansion is always determined by $\rho_+(d)$ (and its complex conjugate $\rho_-(d)$). Since $18/8 < d_c < 16/7$ the sequence of special points d_s ends at $d_s = 16/7$. As we decrease d further towards 2 one discovers that $d = 2$ is a logarithmic singular point for $\rho_+(d)$. Hence, one may encircle $d = 2$ in various ways before changing d further. The figure displays the two behaviors when d is decreased to 0 (after encircling $d = 2$ by angles $\pm\pi$). In one case the singularity moves to $\rho = -1$ when $d \rightarrow 0$, which is a logarithmic singularity of the $d = 0$ equation of state. In the other case ρ_+ moves to $\rho = 0$ when $d \rightarrow 0$. There is no singularity at $\rho = 0$ in the $d = 0$ equation of state, but it is possible for two square root singularities to annihilate when they coalesce. Finally, the figure shows the behavior when $d = 2$ is encircled by 2π , and increased back to $d = 3$. In this case ρ_+ move to $\rho = 0$, where it appears to annihilate with ρ_- . Thus, the analytically continued equation of state has singularities close to $\rho = 0$ when d is close to 3 and 0, but not for d exactly 3 or 0.

m	a_m	α_m
0	0.489 092 994 674 599	-0.115 262 558 466 782
1	0.807 395 011 652 565	-0.639 351 821 397 655
2	3.094 390 113 185 892	-1.159 038 217 120 639
3	17.394 603 934 793 184	-1.466 809 677 404 770

TABLE 1. Numerical parameters for the asymptotic expansion of virial coefficients A_n in 3 dimensions. Equation (7.3), with $|\rho_+| = \exp(2.921\,309\,400\,394\,924)$ and $\omega = 0.710\,413\,678\,806\,621$, provide an accurate representation for large n . The relative error in A_n when summing the series in (7.3) to $m = k$ can be expected to be of order $n^{-(k+1)}(a_{k+1}/a_0)$.

We insert this expansion for the pressure into the integral expression (4.5), and deform the integration contour around the square root branch cut starting at $\rho = \rho_+$. Writing $\rho = \rho_+(1+t)$ gives a contribution

$$\begin{aligned} A_n^{(+)} &= \frac{1}{\pi} (2/r_2)^{1/2} \rho_+^{3/2-n} \int_0^\infty \frac{dt t^{1/2}}{(1+t)^{n+1}} + \dots \\ &= \frac{1}{\sqrt{2\pi} r_2} \rho_+^{3/2-n} n^{-3/2} + \dots \end{aligned}$$

to (4.5). There is a similar contribution $A_n^{(-)} = A_n^{(+)*}$ from the singularity at ρ_- . There are also higher order contributions from weaker singularities (proportional to $\Delta\rho^{m+1/2}$) in Δp . This leads to the following expansions

$$\begin{aligned} A_n &\approx |\rho_+|^{3/2-n} \sum_{m=0} c_m \cos(\omega n + \phi_m) \int_0^\infty \frac{dt t^{1/2+m}}{(1+t)^{n+1}} \\ &= n^{-3/2} |\rho_+|^{3/2-n} \sum_{m=0} n^{-m} a_m \cos(\omega n + \alpha_m), \end{aligned} \quad (7.3)$$

with amplitudes a_m , c_m and phases α_m , ϕ_m which are straightforward to compute. The first numerical values of a_m and α_m for dimension $d = 3$ are listed in table 1.

Because of the oscillatory behavior, it is difficult to find an accurate asymptotic fit to A_n directly from the numerical series, in particular if the prefactor $n^{-3/2}$ is unknown. In retrospect one realizes that this n -dependence is the generic behavior of the algebraic prefactor, due to the square root type of the singularity (7.2).

8. BEHAVIOR AT THE BOSE-EINSTEIN CONDENSATION POINT

To understand why the dimensions d_m are special for the virial expansion, with a radius of convergence much larger than ρ_{BE} , we must investigate the equation of state for ρ near ρ_{BE} . The formula (5.4) is useful for this. We restrict analysis to the interval $2 < d < 4$. It follows that

$$\begin{aligned} (\rho_{\text{BE}} - \rho) &= -\Gamma\left(1 - \frac{1}{2}d\right) (-\mu)^{-1+d/2} + \dots, \\ (p_{\text{BE}} - p) &= \zeta\left(\frac{d}{2}\right) (-\mu) + \dots, \end{aligned}$$

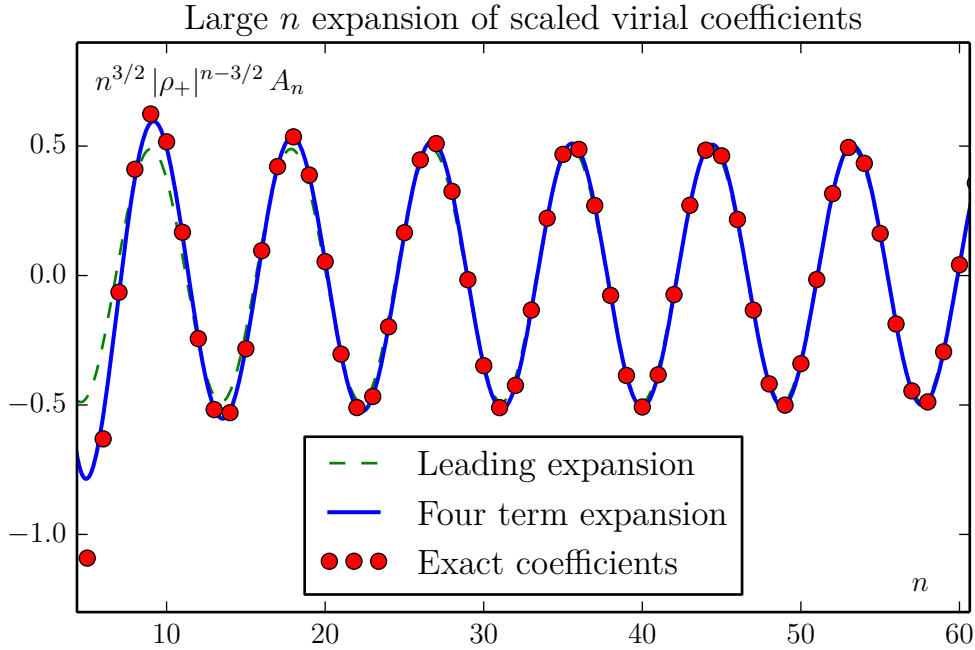


FIGURE 9. The exactly computed values of scaled virial coefficients compared with the expansion (7.3). The expansion does not work well for low n , due to contributions from additional singular points (further away from the origin) of the equation of state.

as $\mu \rightarrow 0^-$, with $\rho_{\text{BE}} = \zeta(\frac{d}{2})$ and $p_{\text{BE}} = \zeta(1 + \frac{d}{2})$. Elimination of μ gives the equation of state as $\rho \rightarrow \rho_{\text{BE}}$ from below:

$$(p_{\text{BE}} - p) = \rho_{\text{BE}} \left[\frac{(\rho_{\text{BE}} - \rho)}{-\Gamma(-1/\delta)} \right]^\delta + \dots, \quad (8.1)$$

where $\delta = 2/(d-2)$. This term is non-singular when δ is equal to an integer $1+m > 1$. This corresponds to dimensions $d = 2 + 2/(m+1)$ with $m = 1, 2, \dots$, giving $p_{\text{BE}} - p \sim (\rho_{\text{BE}} - \rho)^{m+1}$. For odd m this equation of state is obviously unphysical when $\rho > \rho_{\text{B}}$, but this is not equally obvious when m is even. There is, however, a signature of singular behavior in the density fluctuations, which diverge like $(\rho_{\text{BE}} - \rho)^{-m}$.

One must also check that there are no singularities to higher orders. For this it follows from equation (5.4) that p and ρ are analytic functions of $\xi \equiv (-\mu)^{1/\delta}$ in a region around $\mu = 0$ (the power series converges), with $d\rho/d\xi \neq 0$ at $\xi = 0$. Therefore, the function $\rho(\xi)$ can be inverted. This implies that ξ , $\mu = -\xi^\delta$, and p are analytic functions of ρ in some region around ρ_{BE} for all special dimensions given by equation (3.2). However, this does not necessarily imply that there will be a sudden increase of the convergence radius of the virial expansion at these dimensions, since the convergence may be governed by singularities closer to the origin than ρ_{BE} .

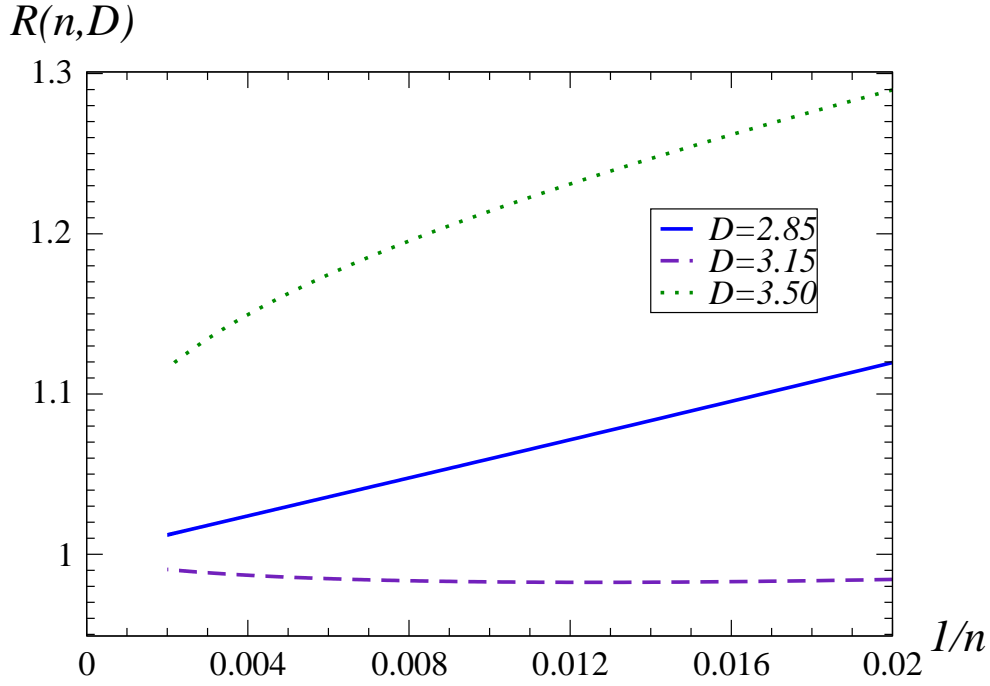


FIGURE 10. The ratios $R(n, d) = A_n(d)/A_n^{\text{BE}}(d)$ as function of n^{-1} , plotted for $n = 50, \dots, 500$. The $A_n(d)$'s are calculated numerically (using 750 decimals accuracy), and divided by the *leading order* contribution (8.2) to $A_n^{\text{BE}}(d)$. The first correction to this ratio is of order n^{-1} when $\delta > 1$ (i.e. for $d < 3$), and of order $n^{1-\delta}$ when $\delta < 1$. It is straightforward to calculate such corrections, but they are best read by computers.

Returning to general dimensions, $2 < d < 4$, we insert equation (8.1) into (4.5) to obtain the asymptotic contribution to the virial coefficients from the Bose-Einstein singularity. By deforming the integration contour around the branch cut starting at $\rho = \rho_{\text{BE}}$ and performing the integration, we find

$$A_n^{(\text{BE})}(d) = \mathcal{B}(d) B(1 + \delta, n - \delta) \rho_{\text{BE}}^{1+\delta-n} + \dots \quad (8.2)$$

as $n \rightarrow \infty$. Here $B(1 + \delta, n - \delta)$ is the beta function, it behaves like $n^{-(1+\delta)}$ as $n \rightarrow \infty$. The coefficient in front is

$$\mathcal{B}(d) = \frac{1}{\pi} [-\Gamma(1 - d/2)]^{-\delta} \sin(\pi\delta). \quad (8.3)$$

The Gamma function has a pole singularity as $d \rightarrow 4$ (i.e. $\delta \rightarrow 1$), cancelling the zero in $\sin \pi\delta$. Thus, the equation of state is nonanalytic at ρ_{BE} for $d = 4$ (which corresponds to $m = 0$ in equation (3.2)). This can also be seen by direct analysis of the equation of state for $d = 4$.

We have checked the accuracy of (8.2) for a few non-special dimensions, see figure 10. The higher order corrections have the form of a double series in powers of n^{-1} and $n^{1-\delta}$. Since

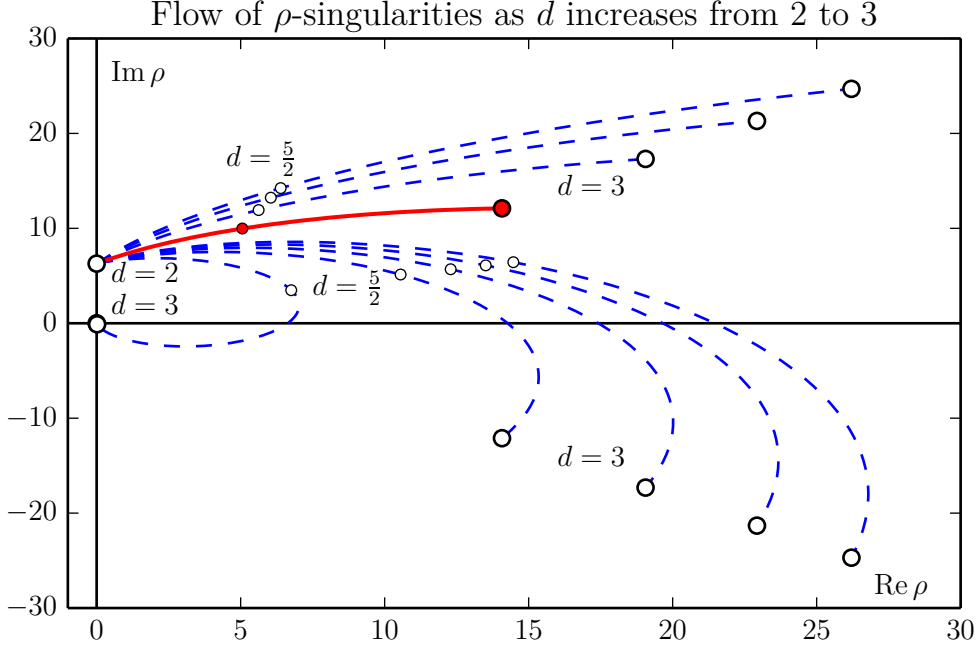


FIGURE 11. This figure illustrates how a few (out of an infinite number) of singularities flow away from $\rho = 2\pi i$ as d is increased from 2 to 3. There is a similar flow related by complex conjugation and $k_0 = 1 \rightarrow k_0 \rightarrow -1$. For exactly $d = 3$ the latter distinction vanishes: The generically logarithmic singularities at $\mu = 2\pi im$ become square root singularities at exactly $d = 3$. As a consequence a translation symmetry under $k \rightarrow k + 2$ emerges. For this reason the apparent singularity at $\rho = 0$ for $d = 3$ is probably annihilated by its complex conjugate, and thus not present at $d = 3$.

$\delta \rightarrow 1^+$ as $d \rightarrow 4^-$ the convergence towards (8.2) becomes slow near $d = 4$, as demonstrated by the $d = 3.5$ case in Fig. 10.

It is now easy to understand why $A_n(d) = 0$ for $d \approx d_m$. The contribution from (8.2) vanishes like $(d - d_m) \rho_{\text{BE}}^{-n}$. It can be cancelled by the contribution from the singularities at ρ_{\pm} . The latter behaves like $|\rho_{\pm}|^{-n} \cos(n\omega + \phi)$. Hence (ignoring algebraic prefactors) there will be a zero when

$$d - d_m \sim \left(\frac{\rho_{\text{BE}}}{|\rho_{\pm}|} \right)^n \cos(n\omega + \phi). \quad (8.4)$$

9. EXPLORING DIMENSIONALITY

For general dimension ρ_+ (and similar singularities) is determined by equation (6.1). Since we know a complex conjugate pair of solutions for $d = 3$, defined by $(\mu_+, k_0 = 1)$ and $(\mu_- = \mu_+^*, k_0 = -1)$, it is straightforward to explore how they move with changing dimension, by changing d in small steps and changing \mathbf{k} when branch cuts are crossed. A map of this exploration (in the z -plane) is shown in Fig. 7, and described in the last part

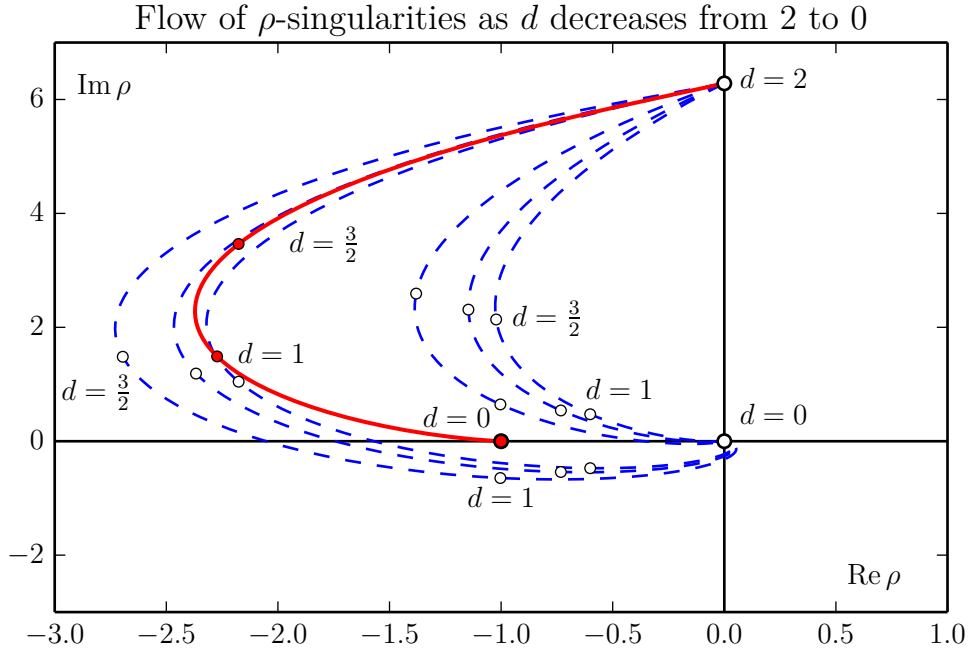


FIGURE 12. This figure illustrates how a few (out of an infinite number) of singularities flow away from $\rho = 2\pi i$ as d is decreased from 2 to 0. There is a similar flow related by complex conjugation.

of its caption. As $d = 2$ the singularity approaches $z = 0$, which in this case corresponds to $\rho = 2\pi i$. The latter can be seen in Fig. 8, where a map of the same curve is shown in the ρ -plane.

Actually, when approaching $d = 2$ one encounters a puzzle. The singularity $\rho_+(d)$ is generally of square root type, with two Riemann sheets attached locally. However, for $d = 2$ it is logarithmic with infinitely many attached Riemann sheets. How can a square root singularity suddenly turn into a logarithmic one? The answer is that this is impossible for a single square root, but it may be possible if we have infinitely many of them. Hence, one must conclude that there are infinitely many ρ -plane singularities approaching $2\pi i n$ when $d \rightarrow 2$. They are actually easy to locate by direct analysis of equation (6.1). They correspond to $\text{Re } \mu \sim \log |d - 2|$, and values of $\text{Im } \mu$ which change in steps of approximately 2π .

A simple way to generate them numerically is to follow the solution as d encircles $d = 2$ in the plane of complex dimensions, $d = 2 + \delta e^{i\phi}$ with some small positive δ . Note that equation (6.1) has only pole singularities as function of d , hence each circle leads back to the same equation. However, each change of ϕ by 2π leads to a new solution. Having generated many new singularities this way one may again follow their paths back to $d = 3$. This is shown in Fig. 11.

Similarly, we may change ϕ to $\phi + (2n + 1)\pi$ for various n , and see how the singularities flow when we decrease d from $2 - \delta$ towards $d = 0$. This is illustrated in Fig.12. To our

initial surprise, most singularities (probably infinitely many — all but one) flow towards $\rho = 0$. On the other hand, we know from the explicitly found equation of state at $d = 0$ that there is no singularity at $\rho = 0$ on any Riemann sheet. Hence, it must be that they annihilate at $d = 0$. By direct analysis of the equation it is possible to see that there must be an infinite number of solutions to (6.1) approaching $\rho = 0$ as $d \rightarrow 0$. The analysis is similar to the one for $d = 2$. We have not investigated the “annihilation process” in detail. Another surprise is that only one square root singularity flows toward the logarithmic one at $\rho = -1$ for $d = 0$ (there is one more related by complex conjugation). The infinity of additional singularities needed to build a logarithmic one must flow from the other $d = 2$ singular points $2\pi im$.

10. SUMMARY AND CONCLUSIONS

In this paper, we have investigated the analytical structure of the virial expansion and equation of state of ideal quantum gases in arbitrary (real-valued) dimensions, with an emphasis on locating the singularities that determine the radius of convergence of the expansion. These simple systems have a surprisingly rich complex analytical structure.

When investigating the behavior near $d = 3$, one finds that *we live in a very special dimension* from the point of view of the virial expansion. Namely, for d close to 3 the equality $\rho_c(d) = \rho_{\text{BC}}(d)$ holds for every $d \neq 3$, but *not* for exactly $d = 3$. The virial coefficients $A_n(d)$ have zeros which approach $d = 3$ very rapidly as n increases. This leads to a sudden increase of the convergence radius at exactly 3 dimensions, paradoxically extending the radius of convergence far beyond the critical density for Bose-Einstein condensation (in the bosonic case). Enlarging the investigations to a wider d -range, one finds the same behavior at a few other special dimensions d_m . There are six such cases in all, $d_m = 2 + 2/(m + 1)$ for $m = 1, 2 \dots 6$. We have revealed a rich analytical structure in the virial expansion, when suitably extended to the complex plane, that explains this behavior.

When searching for the complex conjugate pairs of singularities which determine $\rho_c(d_m)$, we find that they are determined by the simple equation (6.2) in $d = 3$ dimensions, and more generally by equation (6.1).

While we have focused exclusively on noninteracting quantum gases in this paper, we expect that some of the results may be extended to interacting cases. Interacting systems where mean-field theories are applicable (that is, above some lower critical dimension) are essentially effective single particle problems and as such may fall within the class of problems we have considered here, provided that the resulting mean-field theory features long-lived excitations above the ground state condensate which are either fermionic or bosonic. Mean field theories go beyond any order in perturbation theory and often capture interesting physics of strong-coupling fixed points. They tend to be exact as the dimension approaches an upper critical dimension. In this context, we note here that the effective dimension d is twice the dimension of physical space in the relativistic cases. Low-energy excitations of quantum spin systems defined on fractal lattices may also be described by dilute Bose gases with noninteger d .

A.S. was supported by the Research Council of Norway, through Grants 205591/V20 and 216700/F20.

REFERENCES

- [1] J.E. Mayer, *Encyclopedia of Physics*, vol. XII p. 174 (Springer-Verlag, Berlin, 1958).
- [2] S.N. Bose, *Zeitschrift für Physik* **26**, 178 (1924).
- [3] A. Einstein, *Berliner Berichte* 261 (1924); *ibid* 3 (1925).
- [4] E. Fermi, *Rend. Lincei* **3**, 145 (1926); for an English translation see arXiv:cond-mat/9912229.
- [5] P.A. Dirac, *Proc. Roy. Soc. London* **112**, 661 (1926).
- [6] A short communication of parts of this work was presented at Statphys 20: Book of abstracts T0365:SC01/21 (1998).
- [7] W.H.J. Fuchs, *J. Rat. Mech. Anal.* **4**, 647 (1955).
- [8] B. Widom, *Phys. Rev.* **96**, 16 (1954).
- [9] Ø.O. Janssen and P.C. Hemmer, *Phys. Lett.* **35A**, 149 (1971).
- [10] R. Ziff and J.M. Kincaid, *J. Math. Phys.* **21**, 161 (1980).
- [11] D. Sen, *Nucl. Phys.* **B360**, 397 (1991).
- [12] S. Viefers, *Statistical Mechanics of Anyons in the Mean Field Approximation* Cand. scient. thesis (University of Oslo, 1992).
- [13] S. Viefers, F. Ravndal and T. Haugset, *Am. J. Phys* **63**, 369 (1995); hep-th/9408011.
- [14] J.E. Mayer, *Encyclopedia of Physics*, vol. XII p. 174 (Springer-Verlag, Berlin, 1958).
- [15] F.D.M. Haldane, *Phys. Rev. Lett.* **67**, 937 (1991).
- [16] M.V.N. Murthy and R. Shankar, *Phys. Rev. Lett.* **73**, 3331 (1994).
- [17] S. Ouvry and A.D. de Veigy, *Phys. Rev. Lett.* **75**, 352 (1995).
- [18] A. Erdélyi (editor), *Higher Transcendental Functions*, vol. I sect. 1.11 (McGraw-Hill, New York, 1953).

INSTITUTT FOR FYSIKK, NORGES TEKNISK-NATURVITENSKAPELIGE UNIVERSITET, N-7491 TRONDHEIM, NORWAY

E-mail address: Kare.Olaussen@ntnu.no

INSTITUTT FOR FYSIKK, NORGES TEKNISK-NATURVITENSKAPELIGE UNIVERSITET, N-7491 TRONDHEIM, NORWAY

E-mail address: Asle.Sudbo@ntnu.no